Quality factor in *a*-Si:H *nip* and *pin* diodes

C. van Berkel, M. J. Powell, A. R. Franklin, and I. D. French
Philips Research Laboratories, Redhill, Surrey RH1 5HA, England

(Received 15 September 1992; accepted for publication 26 January 1993)

We analyze the forward characteristics of *a*-Si:H *nip* and *pin* diodes. At low bias, a well-defined exponential region exists, described by a noninteger quality factor n between 1.2 and 1.7. With increasing temperature, the quality factor decreases. This behavior can be understood with a model based on electron and hole recombination in the *i* layer, which relates the temperature dependence of the quality factor to the distribution of localized states in the amorphous silicon. The predictions of the model are supported by numerical calculations in which the diode device equations are solved for a given distribution of localized states. The different ideality factors are due to different energy dependencies of the density of deep states in the *i* layer.

INTRODUCTION

Amorphous silicon (*a*-Si:H) diodes are becoming of increasing interest as switches in active matrix addressing of liquid crystal displays (LCDs).[1–5] For such applications, we are interested mainly in the dark diode characteristics and, depending on the way in which the diodes are used, different parts of the *I–V* curve are of prime importance. For instance, in the diode ring scheme[1] and in related schemes,[4] the forward characteristics are important, while in others[5] good reverse characteristics also play a major role. In this article, we look at the dark forward characteristics of *nip* and *pin* diodes and their temperature dependence.

The conduction mechanisms in *a*-Si:H diodes have been analyzed extensively in the literature. Two components to the dark forward current have been identified, drift/diffusion and recombination.[6] The former consists of carriers that diffuse over the potential barrier and recombine in the doped layers and has a quality factor close to unity, while the latter consists of carriers that recombine in the intrinsic layer in a Shockley–Read–Hall (SRH) process and gives a quality factor near 2. Under illumination, drift/diffusion and recombination processes were related to the open circuit voltage of solar cell diodes, with recombination limiting the open circuit voltage of diodes with high built-in potential.[7] Tunneling at the *p/i* interface has also been considered, particularly as a mechanism limiting the open circuit voltage.[8,9] The exact nature of the tunneling process is unclear, with some articles speculating that hole[9] and others that electron[8,10] tunneling takes place. The temperature dependence of the dark diode quality factor has also been taken as evidence for tunneling,[9] analogous to heterojunctions,[11] and *c*-Si Schottky diode behavior.[12] Tunneling models, however, require the existence of sharp interfaces, with high densities of recombination centers strongly localized at the interface. We believe that such states are unlikely to exist at interfaces between a doped and undoped layer, and we know of no strong evidence for their existence. In fact, we do expect the densities of Si dangling bond states in the *i* layer to increase as we move towards the *p–i* and *n–i* interfaces, since the equilibrium density of Si dangling bond states increases as the Fermi level is displaced from midgap.[13,14] However, although this effect will modify the densities of deep localized states, the expected change in the band-bending profile is not so dramatic that it modifies the conduction mechanism, and we do not expect this to lead to a significant tunneling current. In this article, we do not include this effect and we take the density of states to be homogeneous in the *i* layer.

We present in this article, a model in which the diode current is determined by SRH recombination through a spatially homogeneous distribution of deep states in the *i* layer. Computer simulations based on such a model, successfully simulate the observed temperature dependence of the diode quality factor.[15] We present results on *nip* and *pin* diodes and in the analysis provide a physical picture for a noninteger quality factor and its temperature dependence.

EXPERIMENTS

The experiments were performed on two types of diodes, *nip* and *pin*. The letters indicate the order in which the layers were deposited in a multichamber plasma enhanced chemical vapor deposition (PECVD) system. The *i*-layer thickness was 1 μm for the *nip* and 0.5 μm for the *pin*. *I–V* characteristics of both types of diode at different temperatures are shown in Figs. 1 and 2. Measurements were done on 1 mm^2 *nip* and 0.25 mm^2 *pin* diodes. At these sizes, both forward and reverse characteristics show good scaling with area and the results have been plotted in A/cm^2.

At each temperature, the characteristics contain a well-defined exponential regime described by

$$I = I_s \exp\left(\frac{qV_a}{nkT}\right) \tag{1}$$

in which I_s is the saturation current and n the quality factor. The quality factor as a function of temperature is shown in Fig. 3. As can be seen the quality factor for *pin* diodes is significantly larger than for *nip* diodes, but in both cases the quality factor decreases with increasing temperature. The full lines in Fig. 3 represent fits from a model that will be discussed later.

 0021-8979/93/105264-05$06.00

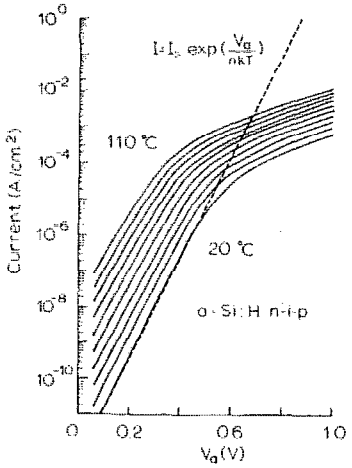

FIG. 1. Experimental I–V curves of a 1 mm^2 *nip* diode measured at 20 °C intervals.

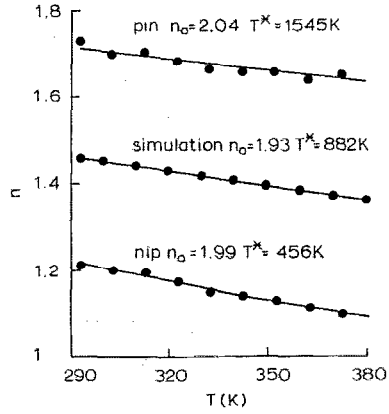

FIG. 3. Diode quality factor as function of temperature for the *nip* and *pin* diodes in Figs. 1 and 2, respectively and for the computer simulated I–V curves in this figure. Full lines represent fits to Eq. (7).

COMPUTER SIMULATIONS

A computer program has been developed to model the diode behavior by solving the relevant device equations numerically. The program uses standard library subroutines to solve in sequence, Poisson's equation, and each of the electron and hole continuity equations.[6,15,16] The sequence is repeated until a consistent result is obtained. An empirical distribution of localized states was used, which was built up out of linear band tails and exponential distributions of deep states. The charge density in Poisson's equation is calculated using standard expressions for the occupancy under a nonequilibrium steady state.[17] The recombination term in the continuity equations was given by SRH recombination integrated over the density of states.[17] No tunneling terms were included in the modeling. The drift/diffusion current was included in the modeling by using doped bulk carrier densities in the n^+ and p^+ regions as boundary conditions for the continuity equations. Typical I–V curves produced with this program are shown in Fig. 4. Like the experimental results in Figs. 1 and 2, the simulated characteristics have well-defined noninteger quality factors at low bias and display space charge limited current behavior at higher bias. The quality factors of the simulated I–V curves are also shown in Fig. 3. The parameters for the simulation shown here were chosen to give values of the quality factors intermediate to the experimental *nip* and *pin* results. Close fits with each of the experimental results could be obtained by adjusting the appropriate parameters.

Important parameters used in the computer modeling were *i*-layer thickness 1 μm; the minimum in the density of states was located 0.65 eV below the conduction band. The density of states at the minimum was 10^{15} cm^{-3} eV^{-1}, and the characteristic temperature above the minimum was 900 and 514 K below the minimum. The importance of these parameters is discussed in more detail in the next section. Carrier capture cross section and thermal velocity product $\sigma v = 8\times10^8$ cm^3 s^{-1}. As mentioned, linear band tails were used with a 0.133 eV width for the conduction band tail

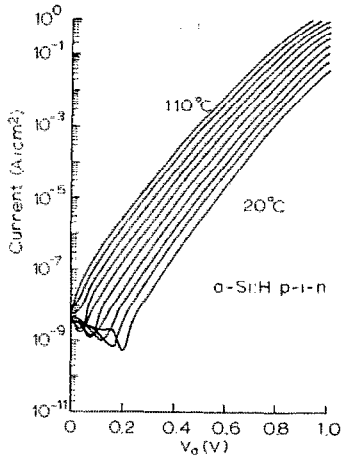

FIG. 2. Experimental I–V curves of a 0.25 mm^2 *pin* diode measured at 20 °C intervals.

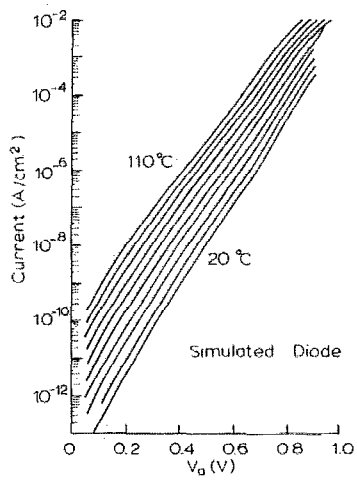

FIG. 4. Simulated I–V curves produced by computer calculations.

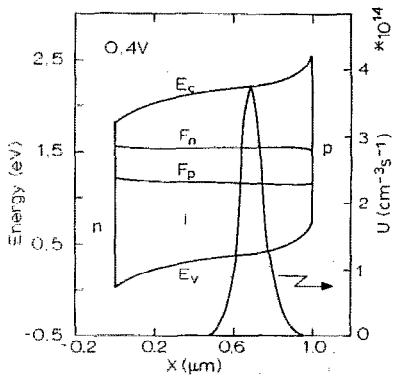

FIG. 5. Modeled diode band bending and electron–hole recombination at 0.4 V bias.

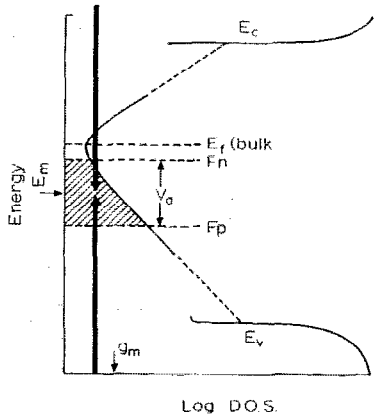

FIG. 6. Schematic representation of the density of states in *a*-Si:H. Indicated are E_f, the Fermi level position in bulk material, and F_n and F_p the electron and hole quasi-Fermi levels. The localized states between the quasi-Fermi levels act as recombination centers.

and a 0.266 eV width for the valence band tail. The free-carrier mobilities were $\mu_e=10\ \mathrm{cm^2\,V^{-1}\,s^{-1}}$, $\mu_h=0.1\ \mathrm{cm^2\,V^{-1}\,s^{-1}}$.

PHYSICAL MODEL

Investigation of the numerical results showed that the total current was dominated by recombination in the *i* layer and that there was little contribution of the drift/diffusion current. The numerical results indicate, therefore, that the SRH recombination can result in a noninteger quality factor. How this can be understood physically is discussed in this section. Figure 5 shows the diode band bending and electron–hole recombination in the *i* layer at a forward bias of 0.4 V. The total current is equal to the total amount of recombination in the device, which is given by the area under the recombination curve in Fig. 5;

$$I\sim\int_0^d\frac{Rnp}{Rn+p}\int_{Fp}^{Fn}g(E)dE\,dx. \tag{2}$$

$Rnp/(Rn+p)$ is the SRH recombination,[17] with R the ratio of electron and hole capture cross sections. The SRH recombination occurs through the localized states lying between the quasi-Fermi levels Fp and Fn[17] illustrated by the shaded area in Fig. 6. The second integral in Eq. (2) represents, therefore, the number of states participating in the recombination process.

To reveal the essential physics, Eq. (2) is simplified in two steps, first, we note that the SRH term has a maximum when $Rn=p$, where we can write $Rn=p=\sqrt{Rnp}$. The last quantity is given by the split between the quasi-Fermi levels which is essentially constant throughout the device. Taking the point at which $Rn=p$ as the origin and assuming a *locally* uniform field $E_{n=p}$, we can write for the electron and hole densities,

$$\begin{aligned} n&=\sqrt{np}\exp\left(-\frac{qE_{n=p}x}{kT}\right),\\ p&=\sqrt{np}\exp\left(+\frac{qE_{n=p}x}{kT}\right). \end{aligned} \tag{3}$$

With this, the first integral in Eq. (2) can be evaluated to give

$$I\sim\left(\frac{1}{E_{n=p}}\right)\left[\exp\left(\frac{-E_g}{2kT}\right)\exp\left(\frac{qV_a}{2kT}\right)\right]\int_{Fp}^{Fn}g(E)dE. \tag{4}$$

The second simplification is made through an approximation of the integral representing the number of recombination centers. The distribution of localized states is illustrated in Fig. 6. Within the context of this article, we are mainly interested in the distribution of deep states just below midgap. We assume that in this region, the localized state distribution is given by

$$g(E)=g_m\exp\left(\frac{E_m-E}{kT^*}\right), \tag{5}$$

in which g_m is the density at midgap E_m and T^* the characteristic temperature of the distribution of localized states. Note that g_m and E_m do not denote the minimum in the density of states. The separation between the quasi-Fermi levels is equal to the applied bias V_a and near $n=p$, they are symmetrically placed around midgap. With this, the density of recombination centers as a function of the applied bias can be calculated. The expression for the recombination current then becomes

$$\begin{aligned} I\sim&\left(\frac{1}{E_{n=p}}\right)\left[\exp\left(\frac{-E_g}{2kT}\right)\exp\left(\frac{qV_a}{2kT}\right)\right]\\ &\times\left[kT^*\exp\left(\frac{qV_a}{2kT^*}\right)\right]. \end{aligned} \tag{6}$$

Comparison of this expression with Eq. (1), leads to the conclusion that the quality factor is given by

$$\frac{1}{n}=\frac{1}{n_0}+\frac{T}{2T^*}. \tag{7}$$

With n_0 equal to 2. The full lines in Fig. 3 are fits to this expression, with n_0 and T^* as fitting parameters. The values for n_0 come out very close to 2 as expected. The characteristic temperature T^* was 1545 K for the *pin* result and 456 K for the *nip*. The fitted value for the computer

simulated diode was 882 K, in line with the value of 900 K which had been used in the expression for $g(E)$ in the actual modeling.

Because in the computer program the full SRH expression was used for the recombination, this result validates the simplifications leading to Eq. (7) and underscores that a straight forward model based on recombination in the i layer can be used to explain the temperature dependence of the diode quality factor.

Previously,[18] we used a relation similar to Eq. (7) to describe the quality factor temperature dependence in *nip* diodes and made a connection between the temperature factor in Eq. (7) and the characteristic temperature of the density of states. However, in that analysis, we made this connection via an assumed exponential bias dependence of the term $1/E_{n=p}$ in Eq. (6). This exponential dependence being due to the buildup of space charge in the exponentially distributed density of states. Subsequent close scrutiny of the numerical modeling showed, however, that this effect, although present, is not sufficiently strong to explain noninteger quality factors of less than 1.8, and this has led us to the analysis presented here, where the change in field is assumed negligible compared to the change in the number of active recombination centers. It is interesting to note that the small discrepancy between the temperature used in the modeling and that obtained from the fit to Eq. (7) is probably due to the fact that the fit to Eq. (7) does in fact ignore the local field $E_{n=p}$ dependence on the applied bias V_a, whereas this effect is included in the full computer simulation.

DISCUSSION

We have shown that a physical model based on recombination in the i layer can be used to explain the existence of well-defined noninteger quality factors in both *nip* and *pin* *a*-Si:H diodes. The reason for the noninteger quality factor lies in the fact that the number of deep states acting as effective recombination centers increases exponentially with applied bias. This causes a sharper increase of the recombination current with applied bias, and hence a lower quality factor, than normally associated with recombination processes. The exponential increase in recombination centers is related to the exponential distribution of localized states near the quasi-Fermi level and the quality factor temperature dependence provides a measure of the localized state distribution in that region. It does so, however, over a very limited energy range. As can be seen from Figs. 1 and 2, the exponential forward current region described by Eq. (1) extends over 0.4–0.6 V. Because at $n=p$ the quasi-Fermi levels are placed symmetrically around midgap, this is equivalent to a quasi-Fermi level excursion of merely 0.2–0.3 eV. Hence, the characteristic temperatures derived in the fit to Eq. (7) cannot be said to be representative of the entire distribution of deep states but must instead be limited to a narrow energy range.

A similar comment can be made with respect to the spatial distribution of localized states. In the computer modeling, we have used a homogeneous density of states throughout the i layer. In the actual device, however, we expect the density of states to vary continuously from n/i to the p/i contact as a result of the thermal equilibration of the density of states, that occurs during growth or annealing at temperatures above 200 °C. The fact that the computer program produces results closely resembling the experimental results is due to that fact that forward diode current is sensitive only to the density of states in the region of the device, where the recombination peaks (i.e., where $n=p$). The density of states outside this region may influence the actual space charge, but will have little impact on the recombination itself and the total current. Hence, although the computer program uses a spatial homogeneous density of states outside the area where the recombination peaks, the error introduced by this assumption is small.

The analysis presented here applies to both *nip* and *pin* diodes and it implies that the difference in quality factor commonly observed between the two types of diodes is not due to a difference in conduction mechanism, but rather to a different density of states distribution near midgap in the region where the recombination peaks. The exact origin of this difference requires further examination.

In the past, recombination has been dismissed as a major component of the diode current in favor of tunneling currents, because it was found experimentally that the diode current did not increase linearly with i-layer thickness,[10] while such an increase had been expected for the recombination current.[6] Experiments at our laboratory also show no clear thickness dependence of the forward current regime described by Eq. (1) for a reasonable range of thicknesses. From the simplified analysis of the recombination in the i layer, presented here, and resulting in Eq. (6) we see that the only term from which a thickness dependence might result is the local field at the peak in the recombination distribution, $E_{n=p}$. For instance, if a uniform field is assumed in the i layer, then the field is given by

$$E=\frac{V_a-V_{bi}}{d_i}, \tag{8}$$

and a thickness dependence of the recombination current results. In reality however, significant space charge densities exists near the n/i and p/i interfaces, resulting in significant band bending there, with a region of low charge and low field in the middle of the device as illustrated in Fig. 4. Because intrinsic *a*-Si:H is slightly n type, the recombination peak at $n=p$ does actually occur near the region of significant space charge and band bending near the p/i layer. The band bending here is relatively insensitive to the i-layer thickness. The recombination current is, therefore, independent of i-layer thickness and therefore, the present model *can* account for experimentally observed currents in *a*-Si:H diodes.

[1] S. Togashi *et al.*, Proc. SID **26/1**, 9 (1985).
[2] Y. Baron, A. Lien, V. Cannella, J. Mcgill, and Z. Yaniv, Proc. SID **68** (1986).
[3] H. Sakai, M. Kamiyama, and E. Tanabe, Mater. Res. Soc. Symp. Proc. **118**, 375 (1988).

[4] K. H Nicholas *et al.*, Proc. Eurodisplay **90**, 170 (1990).
[5] K. E. Kuijk, Proc. Eurodisplay **90**, 174 (1990).
[6] I. Chen and S. Lee, J. Appl. Phys. **53**, 1045 (1982).
[7] M. Hack and M. S. Shur, J. Appl. Phys. **55**, 4413 (1984).
[8] T. J. McMahon and A. Madan, Mater. Res. Soc. Symp. Proc. **49**, 287 (1985).
[9] S. Hegedus, N. Salzman, and E. Fagen, J. Appl. Phys. **63**, 5126 (1988).
[10] H. Matsuura, A. Matsuda, H. Okushi, and K. Tanaka, J. Appl. Phys. **58**, 1578 (1985).
[11] W. A. Miller and L. C. Olsen, IEEE Trans. Electron. Devices **ED-31**, 654 (1984).
[12] S. M. Sze, *Physics of Semiconductor Devices*, 2nd ed. (Wiley Interscience, New York, 1981), Chap. 5.
[13] M. J. Powell, C. van Berkel, A. R. Franklin, S. C. Deane, and W. I. Milne, Phys. Rev. B **45**, 4160 (1992).
[14] G. Schumm and G. H. Bauer, Mater. Res. Soc. Symp. Proc. **192**, 189 (1990).
[15] A. Mittiga, P. Fiorini, M. Falconieri, and F. Evangelisti, J. Appl. Phys. **66**, 2667 (1989).
[16] M. Hack and M. Shur, J. Appl. Phys. **54**, 5858 (1983).
[17] G. W. Taylor and J. G. Simmons, Phys. Rev. B **4**, 502 (1971).
[18] C. van Berkel, M. J. Powell, and I. D. French, Mater. Res. Soc. Symp. Proc. **219**, 369 (1991).